Polymer Journal, Vol. 33, No. 4, pp 344—355 (2001)

Moisture Effect on Structure and Mechanical Property of Nylon 6 as Studied by the Time-Resolved and Simultaneous Measurements of FT-IR and Dynamic Viscoelasticity under the Controlled Humidity at Constant Scanning Rate

Shu Mei ZHOU, Kohji TASHIRO,† and Tadaoki II*

Department of Macromolecular Science, Graduate School of Science, Osaka University, Toyonaka, Osaka 560-0043, Japan
**IT Keisoku Co. Ltd., Todaiji-Cho, Takatsuki, Osaka 618-0002, Japan*

(Received November 15, 2000; Accepted January 17, 2001)

ABSTRACT: Time-resolved simultaneous measurement of infrared spectra and complex Young's modulus was made for nylon 6 films by using the combined system of FT-IR spectrometer and dynamic viscoelastometer under the control of humidity scanned at a constant rate and at a constant temperature. The complex Young's modulus of nylon 6 films annealed at various temperatures was found to decrease with increasing relative humidity. This behavior could be reproduced well by applying the complex mechanical model of the crystalline and amorphous phases with the humidity dependence of the amorphous modulus taken into consideration. The moisture effect on the infrared bands of crystalline and amorphous phases was investigated, from which the moisture-induced disordering in the crystalline region was speculated. The complex Young's modulus was measured at the various strain frequencies under the stepwisely-scanned humidity at 35℃, from which the master curves of the real and imaginary parts of the modulus could be produced successfully. The humidity dependence of the thus evaluated shift factor was found to be fitted quite well to the theoretical equation concerning the free volume in the amorphous region. The characteristic features of the dynamic viscoelatometer system used in this experiment were also investigated in detail.

KEY WORDS Humidity / FT-IR / Dynamic Viscoelastometer / Nylon 6 / Hydrogen Bond / Master Curve / Shift Factor / Free Volume /

When we try to investigate the structure and physical properties of polymer materials, the samples are almost always exposed to the environment of a certain relative humidity. The humidity changes quite often hour to hour and day by day, but usually we do not care at all an influence of this humidity on our experimental data. As will be reported here, this effect of humidity on the structure and physical properties of polymers is not negligibly small. It is important and absolutely necessary to clarify this humidity effect in detail.

The reports about the moisture effect on the structure and properties of polymer materials have been made for a long time in the various ways,[1-30] but the number of reports accumulated so far was not large as we expected from the significance of the humidity effect. One of the reasons might come from such a situation that the control of the relative humidity was not necessarily easy. Besides, for the measurement of the humidity effect on the structure and properties, the samples were for a long time soaked into or suspended over a chamber of the constant humidity, which was made by using a concentrated aqueous solution of some inorganic salt, and then were set into the measurement equipment as soon as possible. The measurements were usually performed in an open atmosphere and so had to be carried out in a short time because of the rapid evaporation of the absorbed water from the sample. In order to overcome these difficult points, a new system was recently developed by Ii.[31] He produced a dynamic viscoelastometer which can measure the dynamic mechanical property of a polymer film under the automatic control of the relative humidity and temperature. Kato *et al.* also produced the similar system.[32-34] One of the unique points of Ii's system is to change the relative humidity of the sample chamber at a constant rate, *i.e.*, linearly with time or step-wise, just like the temperature control in the DSC apparatus. Of course the temperature can be changed also in an arbitrary manner under the suitably controlled humidity. As reported in the previous papers,[35-38] we combined a Fourier transform infrared spectrometer to this dynamic viscoelastometer in order to get the useful information on the relationship between the structural change and the mechanical property change as functions of relative humidity and temperature. The details of this system were already described in these papers.

In one of the previous papers we reported the preliminary results on the simultaneous measurement of infrared spectra and dynamic mechanical property of regenerated cellulose by using this system.[39] In the present paper, more details will be described about the measurement results collected for nylon 6 films. In order to know the contribution of the amorphous and crystalline parts in the water absorption process, the samples with different degrees of crystallinity were used. As already mentioned, this new dynamic viscoelastometer system can handle the relative humidity in an arbitrarily chosen manner, we were challenged to measure the complex Young's modulus at the various frequencies by controlling the humidity at a step-scan mode, which lead us successfully to draw the master curves of E' and E'' in a wide frequency range and allowed us to discuss the role of humidity and temperature in the mechanical behavior of nylon 6. Prior to these measurements for nylon 6

†To whom correspondence should be addressed.

films, we needed to clarify the characteristic features of this humidity scanning system which will affect the measurement data more or less, as likely the case of differential scanning calorimeter (DSC) in the thermal analysis. Therefore the results about the characterization of this system will be reported at first in this paper.

EXPERIMENTAL

Samples

Commercially-available nylon 6 film was melted and quenched into liquid nitrogen temperature to get the sample of low crystallinity. The annealed samples were prepared by heat treatment of this quenched film at various temperatures. The thickness of the films was about 18 μm. The samples were evacuated for a long time at room temperature in order to take the absorbed water out of the sample. The water content of the sample was evaluated from the infrared spectra taken at the same time with the measurement of the dynamic viscoelastometer.

Dynamic Viscoleastometer

The details were already mentioned in the previous papers.[35–39] The sample was clamped by a pair of metal holders which were connected directly to the strain gauge and load cell, giving the strain and stress values working to the sample. The sinusoidal deformation was mainly applied to the sample at the frequency of 10 Hz. The change of the sample length was also simultaneously measured in order to evaluate the elongation (or contraction) due to the humidity or temperature effect. These data were transferred to the computer and saved as digitized data. The output data were the real and imaginary parts of the Young's modulus (E' and E'', respectively), $\tan(\delta)$ ($=E''/E'$), and the change of the sample length (Δl). In the present study the measurement was carried out at a constant temperature of 35℃. In the measurement of humidity dependence, the humidity was linearly changed at the rate of 0.3 or 2% relative humidity min^{-1} (RH% min^{-1}). The humidity was controlled by balancing the relative content of dried and wet air and monitored by a humidity sensor. The temperature was controlled by balancing the heater and the cool nitrogen gas.

The frequency dispersion curves of the complex modulus were measured for the melt-quenched nylon 6 film. The relative humidity was changed in a stepwise mode as reproduced in Figure 1a at a constant temperature 35℃. At each relative humidity the strain frequency was changed automatically at equal time span from 63.0 to 39.8, 25.1, 15.8, 10.0, 6.3, 3.98, 2.51, and 1.58 Hz and the corresponding E' and E'' were calculated. The master curves of E' and E'' were obtained by shifting the measured curves suitably along the abscissa or the frequency axis.

Infrared Spectral Measurement

The infrared beam was taken out of the outlet of a Bio-Rad FTS-60 A/896 spectrometer and lead to the sample chamber by using a flat mirror and a curved mirror focused to the sample position. This infrared beam passed through a small hole opened in the wall of the chamber.

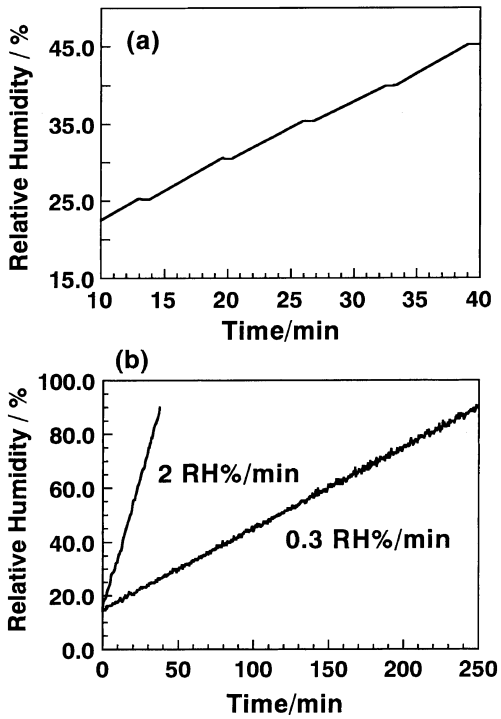

Figure 1. Examples of scanning modes of humidity in the present system. (a) The step-scan mode and (b) mode at constant increasing rates of 2 and 0.3 relative humidity min^{-1}.

The transmitted light was detected by an MCT detector set in the back of the sample chamber. The thus collected signal was sent back to the spectrometer and the Fourier transformation was made in order to get the infrared spectrum. The resolution power of the spectrum was 2 cm^{-1}. The spectrum was measured at every 5 RH% in the scanning process of humidity.

RESULTS AND DISCUSSION

Characteristic Features of the Dynamic Viscoelastometer System under the Controlled Humidity

In the DSC measurement, the melting point, for example, is affected by the heating (cooling) rate of the sample. The total volume of the sample packed in the sample pan is also important because the thermal conduction becomes worse for larger amount of the sample. The present scanning humidity system is considered to have the similar problems. Before discussion of the concrete experimental results, therefore, we investigated the effect of scanning rate and the sample thickness on the humidity dependence of the mechanical properties of nylon 6 films.

Influence of Sample Thickness. Figure 2 shows the humidity dependence of E', E'', $\tan(\delta)$, and the change of the sample length (elongation), which was measured for the melt-quenched nylon 6 films with different thickness of 18 and 33 μm. The scanning rate of relative humidity was 2 RH% min^{-1}. The samples showed the remarkable decrement of the E' in the range of 20—60 RH%, where the E'' and $\tan(\delta)$ showed the broad peaks and the sample length increased gradually. As indicated by vertical lines, the humidity at the maximal E'' and $\tan(\delta)$ shifted slightly toward the higher humidity side for the thicker

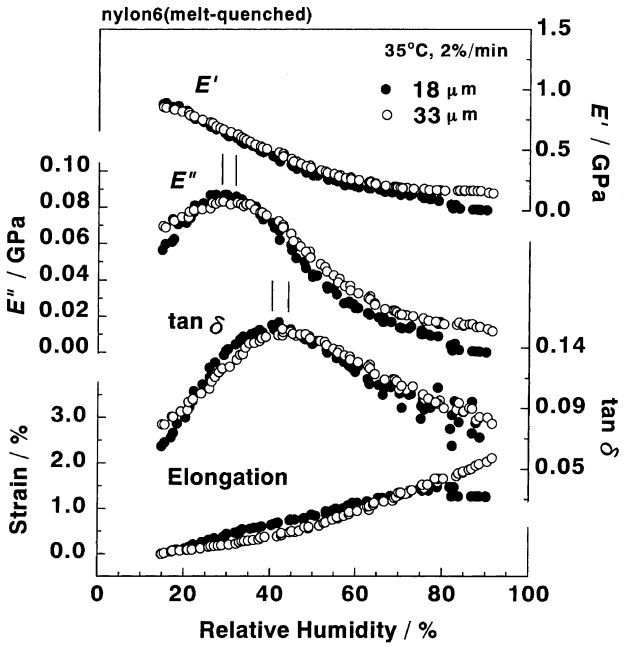

Figure 2. Comparison in the humidity dependence of dynamic modulus (E', E'', and tan δ) and sample elongation between the nylon 6 films with different thickness of 18 and 33 μm.

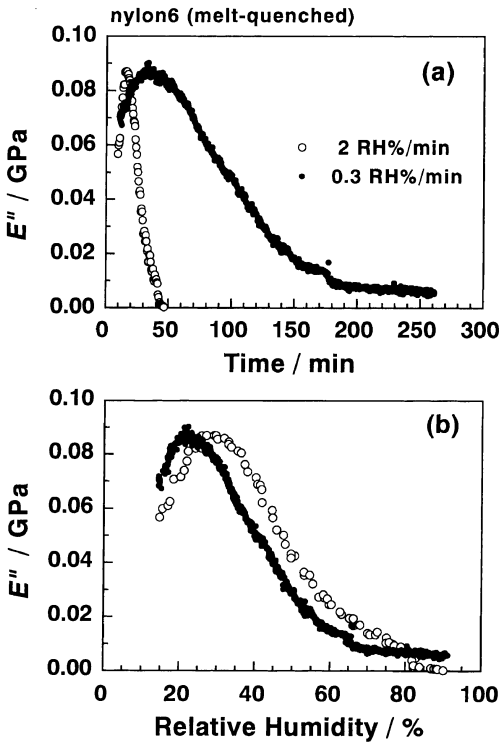

Figure 3. Comparison in (a) the time dependence of dynamic loss modulus E'' of nylon 6 film (18 μm) measured at the different scanning rate of 0.3 and 2.0 relative humidity min^{-1} and (b) the humidity dependence transformed from the curves in (a). Refer to Figure 1b.

sample. The same situation could be detected also for the curves of E' and sample elongation. This phenomenon could be observed with good reproduction and also for such other polymer with different thickness as poly(vinyl alcohol). This shift is interpreted by considering the diffusion of water into the sample from the environmental atmosphere: the time for water to reach the inner part of the sample is longer for the thicker film. This means that the sample thickness must be adjusted exactly when the humidity dependence of the mechanical property is compared between the different samples.

Influence of Scanning Rate of Humidity. Figure 1b shows the time dependence of the relative humidity scanned at 0.3 and 2 RH% min^{-1} at 35℃. In both the cases, the linearity was excellent in the whole range of 15—90 RH%. The mechanical property [E', E'', tan(δ), and sample elongation] was measured in these scanning processes for the melt-quenched nylon 6 films of 18 μm thickness. For example, Figure 3a shows the time dependence of E'' measured at the different scanning rate. At 2 RH% min^{-1}, the maximum of E'' could be detected at about 20 min after starting, while it was about 40 min at 0.3 RH% min^{-1}. Because the linearity of humidity scan was very nice, the curves in Figure 3a could be redrawn almost exactly as the plot of E'' *vs.* humidity. The results are shown in Figure 3b, where a slight but unnegligible difference is detected between the curves measured at the different scanning rates. Lower scanning rate gave the maximal peak of E'' at lower humidity region. If the absorbed water can diffuse and spread instantly over the whole film, then we should not have any time delay even when the scanning rate of humidity is different to some extent. But this cannot be realized in the actual sample. It may be reasonable to ascribe the observed result also to the diffusion of water: the water molecules need some time to spread over the whole sample, causing some time delay when the scanning rate is high. Anyhow the scanning rate of humidity must be adjusted to the same value when the effect of humidity is compared among the various kinds of polymer samples, although the degree of shift of the humidity at the maximal E'' (and tan(δ)) is not very large.

Effect of Tensile Force. In the present system of dynamic viscoelastometer, we apply both the static and dynamic tensile forces to the sample. The static tensile force is for keeping the sample from slackening during the measurement. The dynamic tensile force of sinusoidal form is applied to the sample to measure the dynamic stress–strain relation. The ratio of static to dynamic force was 1.5. At the starting point of the measurement, we apply a static tensile force to the sample. This static force was considered at first to affect the viscoelastic curves as a result of morphic effect, *i. e.*, an effect from the external field. But, in the actual measurement, this initially-applied force was gradually modified so that the ratio of (dynamic force)/(static force) became the preset value. Figure 4 shows this situation clearly. At the time 0 min we started the system. The tensile force and the humidity were adjusted automatically and the measurement was started when the humidity reached the initially-set value and the ratio of (dynamic force)/(static force) was equal to the input value, which occurred about 10 min later since the starting of the system. As the measurement was proceeded, the tensile force became lower. This came from the softening of the sample in the increasing process of humidity as seen in Figure 2: when the sample became softer, the smaller static tensile force was enough to keep the sample from slackening. Even when any static tensile force was ap-

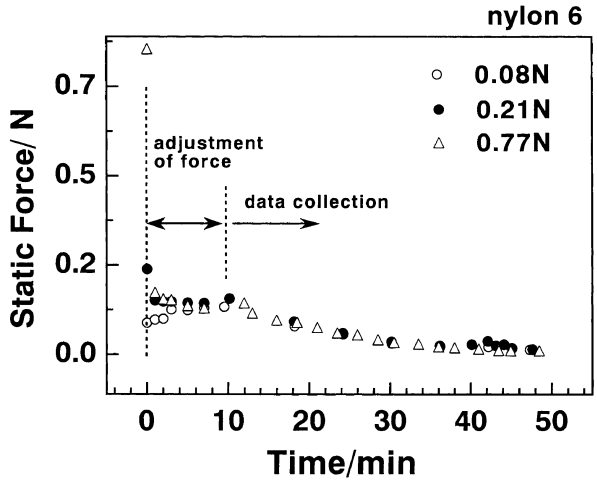

Figure 4. Time dependence of the static tensile force applied to the nylon 6 film in the measurement of humidity dependence of the dynamic modulus.

plied to the sample at the starting point, this roughly applied force was changed to the constant value determined by the preset ratio of (dynamic force)/(static force) at the actual starting point of the measurement (*i. e.*, the starting time of date collection). In this way, the difference in the initially applied tensile force does not give any difference to the measurement result.

Humidity Dependence of Structure and Mechanical Property of Nylon 6

As shown in Figure 5, we measured the humidity dependence of the viscoelastic property of nylon 6 films annealed at the various temperatures. In this measurement the thickness and width of the films were the same within the experimental error. The scanning rate of humidity was 2 RH% min^{-1} and the measurement temperature was 35℃. The Young's modulus E' at the starting point before the sample was exposed to the moisture was higher, of course, for the sample annealed at higher temperature. The E'' was also higher for the annealed sample but the tan(δ) was only slightly different among the samples. All these samples became softer by increasing the relative humidity.[15,18,19] As the relative humidity was increased, the sample was elongated by 1—2% by the effect of tensile force applied lightly to the sample and this elongation became smaller for the annealed sample.

From these experimental data the absorbed water is considered to affect mainly the mechanical behavior of the amorphous region. We tried to simulate the humidity dependence of the Young's modulus shown in Figure 5 on the basis of the mechanical series-parallel model consisting of crystalline and amorphous phases shown in Figure 6.[40,41] Of course we may have various types of models but the model shown in this figure was employed here as a trial. The modulus in the parallel part of crystalline and amorphous regions E_p is given by $E_p = bE_c + (1-b)E_a$, where the parameters (a and b) are defined in Figure 6 and the E_c and E_a are the moduli of the crystalline and amorphous regions, respectively. Therefore the bulk modulus E_{bulk} is expressed by the following eq 1. Since we have the relation of $1/E_{bulk} = (1-a)/E_c + a/E_p$

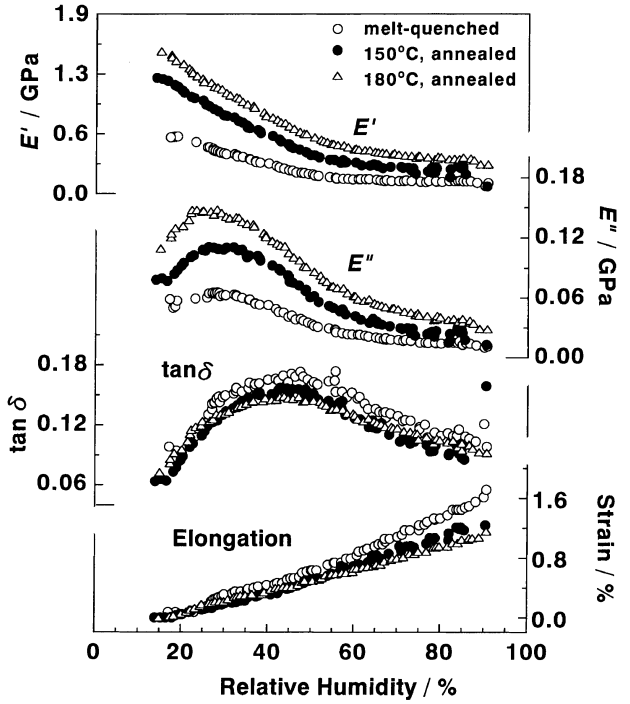

Figure 5. Comparison in the humidity dependence of dynamic modulus (E', E'', and tan δ) and sample elongation between the nylon 6 films annealed at the different temperatures. The increasing rate of relative humidity was 2 RH% min^{-1} at 35℃. The sample films were 18 μm.

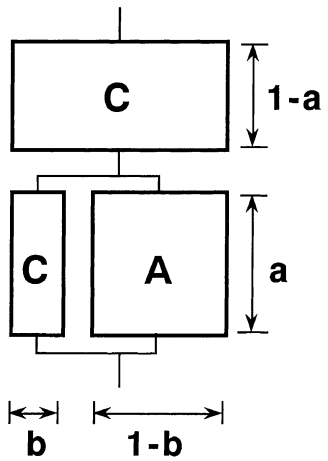

Figure 6. A mechanical series-parallel model used in the calculation of Young's modulus of nylon 6 film. C: crystalline region and A: amorphous region. The parameters a and b are the ratio of C and A as defined in this figure.

for a serial array of the crystalline region (upper part in Figure 6) and the crystalline-and-amorphous parallel region, then

$$E_{bulk} = E_c/\{1-a+aE_c/[bE_c+(1-b)E_a]\} \quad (1)$$

The absorbed water is now assumed to affect the modulus of the amorphous phase in the following mode.

$$E_a = E_a^{\circ} \exp[-m(X_{RH} - X_{RH}^{\circ})] \quad (2)$$

where E_a° is the modulus of the dry state, X_{RH} is the rela-

tive humidity, and m is a coefficient. The amorphous phase is assumed to be affected when the relative humidity becomes higher than some critical value X_{RH}^{o}, at which the water molecules begin to work as a plasticizer. The crystalline region is considered to be affected also by the absorbed water more or less, but the degree is considered to be much smaller than for the amorphous phase, and it is neglected here for simplicity. By carrying out the curve fittings for the E' curves of Figure 5, the parameters a and b are obtained as shown in Table I. In this fitting procedure we input the following numerical values for the various parameters: the $E_c=60$ GPa, which is the averaged values of the crystallite moduli at room temperature estimated along the unit cell axes[42–46] (*ca.* 20 GPa for the a axis, *ca.* 5 GPa for the b axis, and *ca.* 165 GPa for the chain axis), $E_a^{\circ}=1$ GPa, $m=0.06$, and $X_{RH}^{o}=6$ RH%. As shown in Figure 7, the fitting could be made fairly well for all the samples by using the common values for the parameters mentioned above. This suggests that the assumption of the softening of the amorphous region by absorbing water may be reasonable. The negligibly small b values, as listed in Table I, indicate that the mechanical series model is sufficient for the rough description of this mechanical behavior. As seen in Table I, the change of the parameter a is reasonable: the degree of crystallinity is increased by the heat treatment, although the direct quantitative comparison is difficult in the present study.

In this way the present scanning humidity system could show us more clearly the effect of humidity on the mechanical property of the film, compared with the previously reported papers, although the result itself may not be very new. By using this system we could also create the master curves of the frequency dispersion of the Young's modulus, the results of which will be mentioned in a later section.

Table I. Parameters a and b of a Mechanical Series-Parallel Model Determined for Various Nylon 6 Samples

Samples	Melt-quenched	150℃ annealed	180℃ annealed
a	0.88	0.42	0.37
b	0.002	0.002	0.002

Figure 8 shows the humidity dependence of the infrared spectra in the frequency region of 3700—2700 cm^{-1} measured for the melt-quenched nylon 6 film. The OH stretching bands of water are observed in the region of 3700—2700 cm^{-1}. By integrating the band intensity of this region, the relative content of the absorbed water was evaluated. The relation of this band intensity with the mechanical behavior is shown in Figure 9. As the relative humidity of the sample chamber was increased, the absorbed water content increased almost linearly below 40 RH% and showed a deflection point in the 40—50 RH% region, where the tan(δ) showed the broad peak. The wavenumber of the band assigned to the overtone of NH bending mode is also plotted against the humidity. As the water absorption increased, the band position shifted toward higher frequency side, indicating the weakening of the hydrogen bond C=O ... H–N between the amide groups.[16]

In order to investigate the effect of water penetration in more detail, the infrared spectra shown in Figure 8 are analyzed quantitatively. Figure 10 shows a series of the subtracted spectra in the OH stretching region of

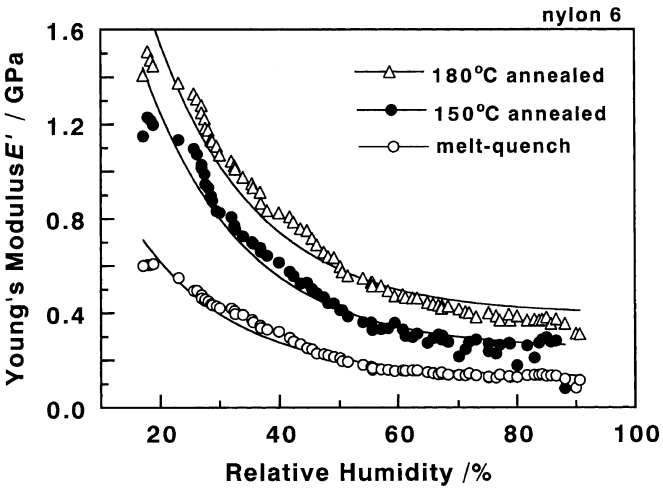

Figure 7. Comparison between the observed and calculated Young's modulus of nylon 6 film plotted as a function of relative humidity.

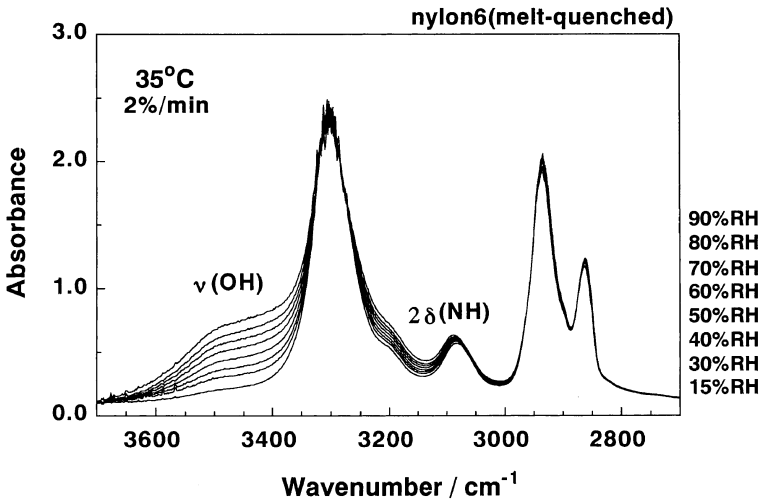

Figure 8. Humidity dependence of infrared spectra of nylon 6 film measured at 35℃ in the course of dynamic viscoelastic measurement.

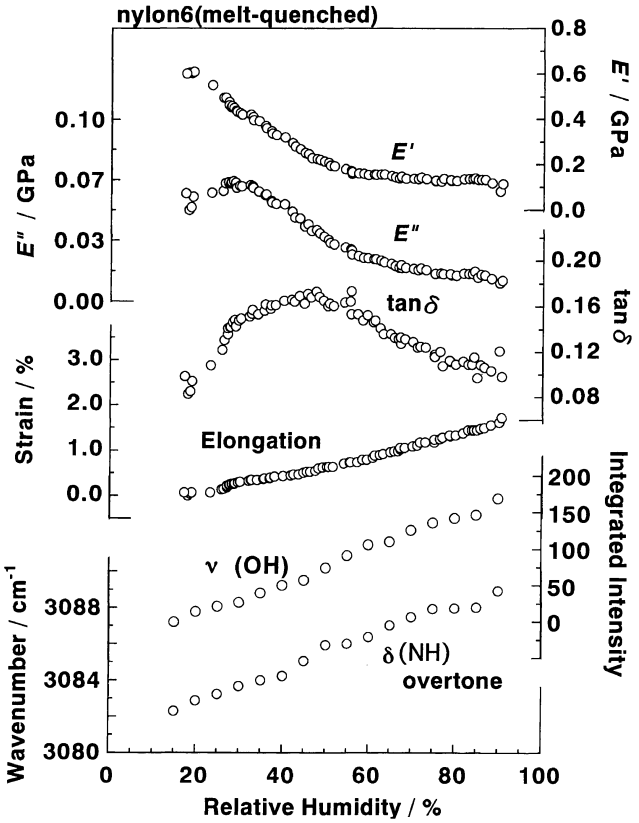

Figure 9. Relation between the observed humidity dependence of the dynamic modulus and the corresponding infrared data (the integrated intensity of water band in 3700—3200 cm^{-1} region and the peak frequency of the overtone band of the NH bending mode) evaluated from Figure 8.

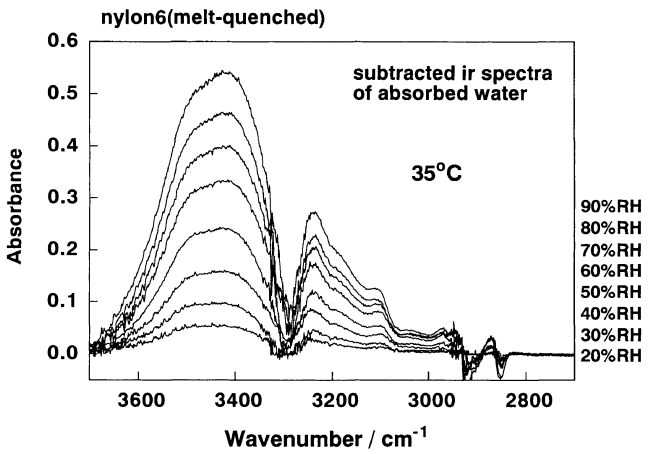

Figure 10. Humidity dependence of the subtracted infrared bands of water absorbed into the nylon 6 film in the frequency region of 3700—2700 cm^{-1}. The subtraction from each spectrum was made by using the infrared spectrum measured at the 15 RH% as a standard.

water molecules, which were obtained by subtracting the spectrum at 15 RH% from the other spectra. The thus obtained spectral profiles of the water band were found to consist of an overlap of plural number of bands. The curve separation into components was made as shown in Figure 11a: the bands were separated into 6 components. These components at the different positions are considered to reflect the different environments of

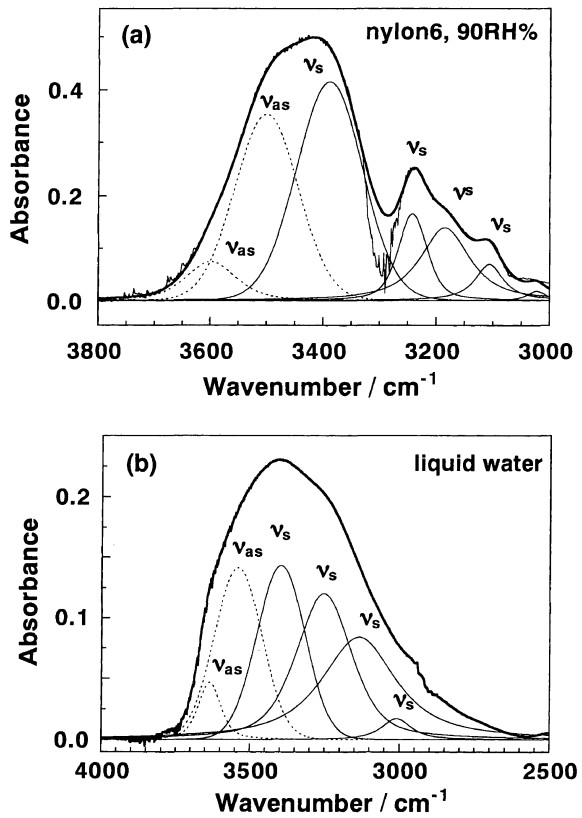

Figure 11. Curve separation for the profile in the frequency region of 3700—2700 cm^{-1}. (a) For the subtracted spectrum of nylon 6 obtained in Figure 10. (b) For the infrared spectrum of liquid water measured at room temperature.

the water molecules or the different strength of the hydrogen bonds.[47] The band assignments to these various states are difficult at the present stage. Even for the basically important liquid water itself, unfortunately, the band assignment has not yet been established because of the complexity of the profile.[48−50] As a trial, we performed the calculation of vibrational frequencies of antisymmetric (ν_{as}) and symmetric (ν_s) stretching modes for the various aggregation states of water, as shown in Figure 12, where the used models were (a) an isolated water molecule, (b) dimer, (c) trimer, (d) tetramer, (e) a cluster of 80 water molecules and (f) a cluster of 384 water molecules. The calculation was made on the basis of classic mechanics (Hessian matrix method[51]) and semi-empirical quantum mechanics (MOPAC version 6) using a commercially available software Cerius[2] (version 4.0, Molecular Simulation Incorporation). These two methods gave the similar results although the absolute values of the vibrational frequencies were slightly different. The result obtained by the Hessian matrix method is shown in Figure 13, where a constructed model was energetically minimized and the molecular dynamics calculation was performed at 300 K under canonical ensemble condition and then the vibrational frequencies were calculated for the thus obtained equilibrium structure. As the number of water molecules included in a cluster is increased, the number of possible models is increased. The spectra calculated for all these models need to be averaged in order to get reliable spectral profiles. Since the results shown in Figure 13 were obtained for only the

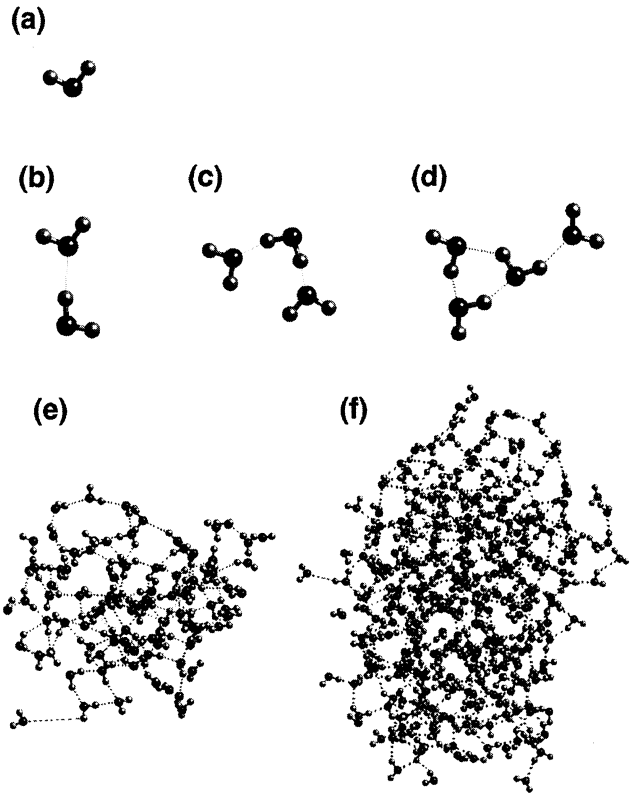

Figure 12. Models of clusters of aggregated water molecules used for the calculation of the infrared spectra: (a) an isolated water molecule, (b) dimer, (c) trimer, (d) tetramer, (e) a cluster of 80 water molecules, and (f) a cluster of 384 water molecules.

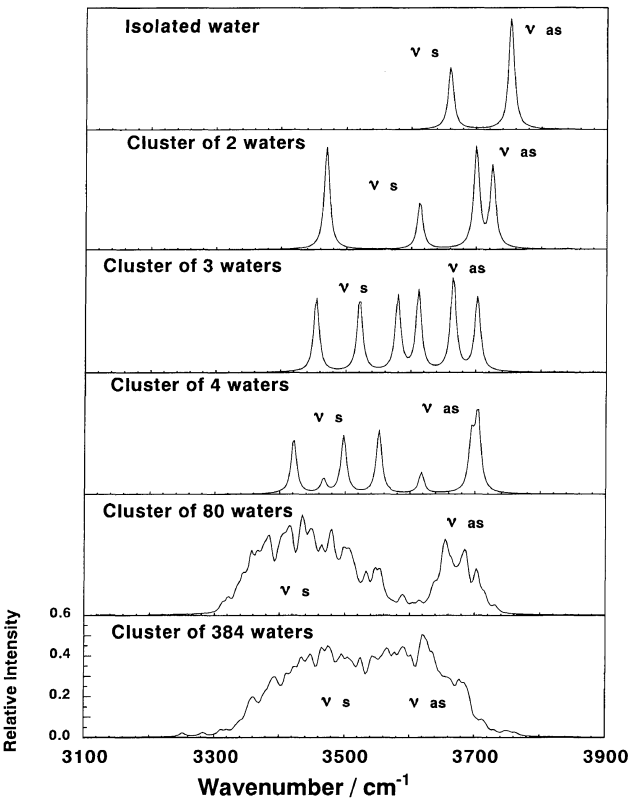

Figure 13. Calculated infrared spectra of water clusters shown in Figure 12.

limited number of possible models (4—5 types of model for one cluster), a quantitative discussion might be difficult at the present stage. But, as for the spectra obtained for several tens of models constructed in this study, at least, we may say that the ν_s band shifts largely depending on the cluster size or the environment of a molecule, while the ν_{as} band position does not shift very much and stays in the frequency region higher than 3500 cm^{-1}. The similar result was reported for hexamer clusters of water.[49] By referring to this result, the subtracted spectra of Figure 10 were separated to the components shown in Figure 11a, which were roughly assigned to the following three groups: the ν_s bands of weakly-bonded (3400 cm^{-1}), moderately-bonded (3240 cm^{-1}), and strongly-bonded water molecules (2 bands in 3180—3100 cm^{-1}). The ν_{as} bands were assumed to appear at almost the constant position of 3600—3500 cm^{-1}. In order to check the reasonableness of this rough classification of the band components, a deconvolution was tried for the infrared spectrum of liquid water. As shown in Figure 11b, the complicated spectral profile could be separated well to these 6 components with small modification of position and relative intensity of each band component. In Figure 14, the integrated intensity of the thus separated band components are plotted against the relative humidity for the nylon 6 sample. All the bands corresponding to the water molecules of different environments were found to increase the intensity almost in parallel with an increase of the relative humidity for the nylon 6 film. Therefore the water absorbed into the nylon 6 film is considered to take the various aggregation forms from weakly-bonded to strongly-bonded state, even at the early stage of absorption. Strictly speaking, however, the band of strongly-bonded water at 3180–3100 cm^{-1} looks to increase more steeply above 40 RH% than the other bands, where the mechanical property showed more remarkable decrease as seen in Figure 9.

As stated above, most of the absorbed water is consid-

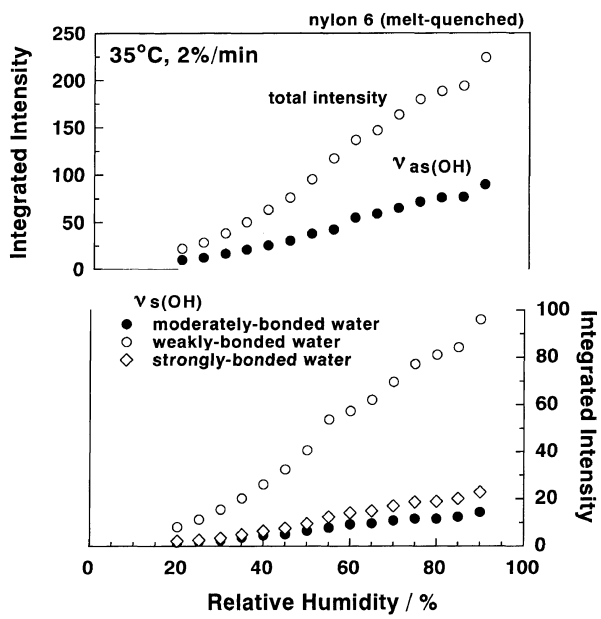

Figure 14. Humidity dependence of integrated intensity of the band components separated from the subtracted spectra of nylon 6 shown in Figure 10.

ered to enter the amorphous region. But the crystalline region should be also affected by the absorbed water, although the relative content of water might be lower. Murthy *et al.* reported the difference in the X-Ray diffraction pattern between the dried and wet nylon 6 samples: the spacing of the sheet planes formed by the hydrogen bonds between the zigzag chains expands by absorbed water.[52] Their measurements, however, were not made *in situ* for the sample exposed in the humid atmosphere. In order to know the behavior of the crystalline and amorphous phases, the infrared spectra taken at the same time with the dynamic viscroelastometry were analyzed. For example, Figure 15 shows the humidity-dependent infrared spectral changes in the frequency regions of (a) 1500—1200 and (b) 900—450 cm^{-1} measured for the melt-quenched nylon 6 film with low crystallinity. The spectra were mainly of the amorphous and crystalline α phases with the small contribution of the crystalline γ phase.[53–56] The amorphous bands are in general quite broad and weak in this nylon 6 sample, and so it is difficult to detect the changes in the position and intensity of the amorphous bands. On the other hand, the crystalline bands are relatively sharp and made it easy to detect their changes. Most clear change is observed for the band at 3086 cm^{-1}, which is assigned to the overtone of N–H bending mode and can be observed only for the crystalline phase, as known from the comparison with the spectrum taken for the molten state. As already shown in Figure 8, this band shifts to the higher frequency side and becomes weaker in intensity with increasing humidity, indicating the decrease of hydrogen bonding strength of the sheet plane by the effect of the absorbed water. As seen in Figure 15, the bands related with the methylene groups in the crystalline region[57] are also observed to decrease their intensity and shift the positions. For example, the CH_2 bending bands at 1463, 1436, and 1419 cm^{-1}, and the CH_2 wagging (and twisting) bands at 1263 and 1239 cm^{-1} decrease the intensity with increasing humidity. The band at 1024 cm^{-1}, assignable to the skeletal CC stretching mode, is shifted to lower frequency side by about 0.5 cm^{-1}, which is a similar behavior observed for this band in the heating process from the room temperature.[58] Although there are many bands which do not show almost any change, the above-mentioned bands seem to be sensitive to the slight change in such environment as humidity and temperature. In particular it is important to notice that these sensitive bands are characteristic of the α crystalline phase and are observed at the different positions from those of the γ phase. This means that these bands are conformation-sensitive bands. Therefore the slight change in the intensity and position of these sensitive bands might be related with the slight change in the molecular chain conformation. If this speculation is correct, we might describe the change in the crystalline structure of nylon 6 α phase as follows. By absorbing water, the distance between the hydrogen-bonded sheets is expanded, as reported by Murthy *et al.*[52] The hydrogen-bond strength is also weakened as seen from the change of amide band position. At the same time the methylene chain segments are also affected, which might be related with a slight disordering in the conformation. Because the spectral change is observed more clearly for the sample of lower crystallinity, these speculated structural change might occur more easily for the sample with relatively loose packing of sheets: they are affected easily by the perturbation due to the absorbed water. Another point to be mentioned here is that we can not say clearly whether the water enters the crystalline lamellae or not, only from these experimental data. The water molecules might attach the surfaces of the lamella, for example, the chain folding surfaces. As a result the surface energy is affected, which results in the slight change in the inter-sheet spacing as well as the chain conformation of the chains in the inner part of lamella. In any way, however, we need to investigate the spectral changes in more detail in order to check the above-mentioned speculation in the structural change.

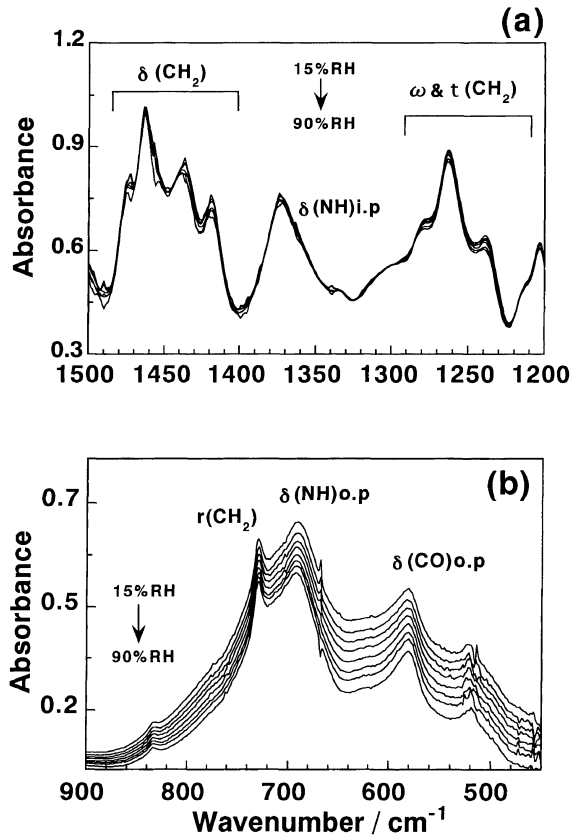

Figure 15. Humidity dependence of infrared spectra of nylon 6 film in the frequency regions of (a) 1500—1200 cm^{-1} and (b) 900—450 cm^{-1}.

Frequency Dispersion of Young's Modulus Affected by Relative Humidity

As mentioned before, the present dynamic viscoelastometer can change the relative humidity in a stepwise manner at a constant temperature, making it possible to measure the complex modulus by changing the applied strain frequency to the various values at each step of humidity. We actually carried out this type of experiment for the melt-quenched nylon 6 film at 35℃. The details of the experimental procedure were described in the experimental section. The thus obtained result is shown in Figure 16, where the E' and E'' at the different humidity are plotted against strain frequency in a double logarithm mode. These curves were found to be reduced to

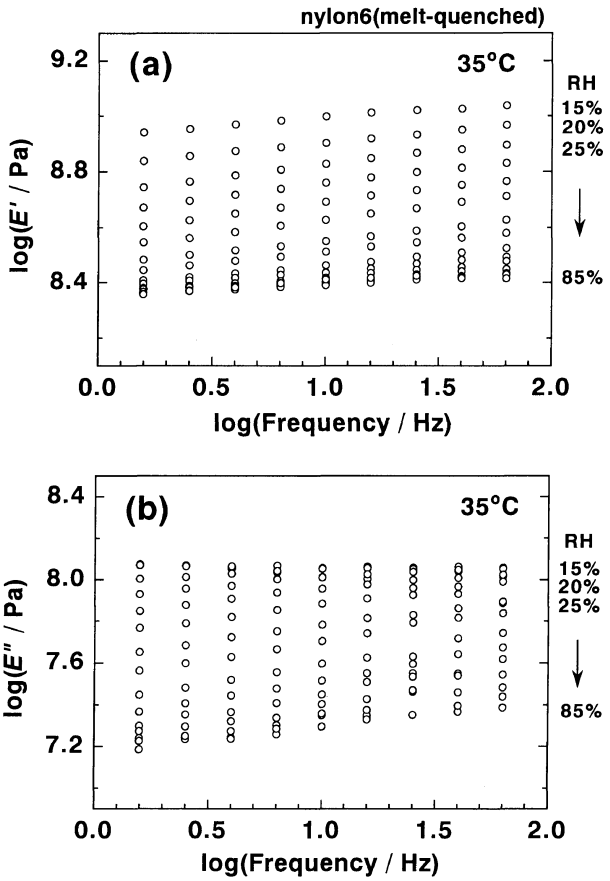

Figure 16. Double logarithmic plot of the Young's modulus E' and E'' *vs.* the strain frequency measured for the nylon 6 film in the step-scanning mode of relative humidity at 35℃ (refer to Figure 1a).

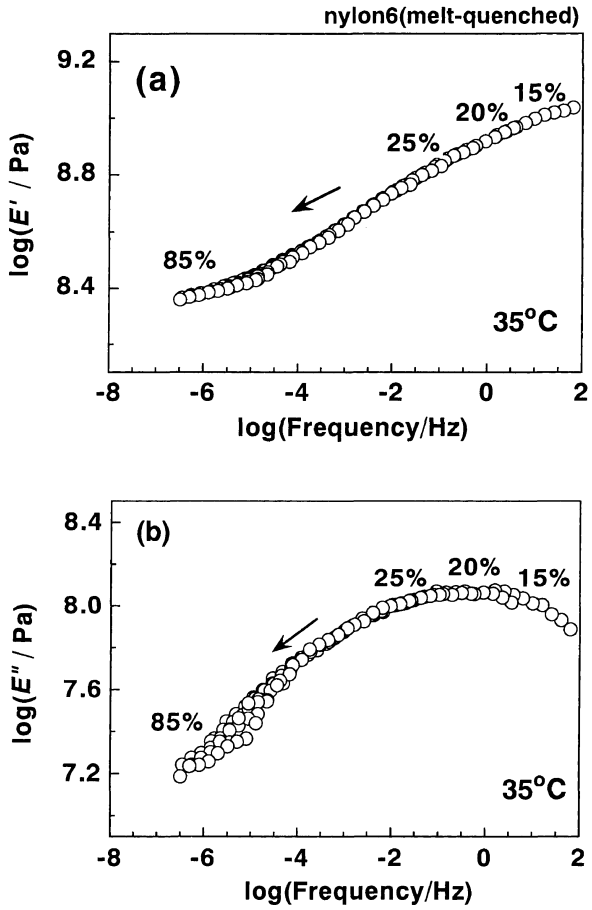

Figure 17. Master curves obtained from the curves given in Figure 16 for E' and E'' of nylon 6 film. The standard state was at 15 RH%.

the master curves by shifting by an appropriate value along the frequency axis. The thus obtained master curves are shown in Figures 17a and 17b for E' and E'', respectively. Similarly to the so-called time-temperature superposition principle, the present experimental result indicates the possibility of the time-humidity superposition. After we completed this experiment for the nylon 6 film, we noticed that this time-humidity superposition was already pointed out for amorphous poly(vinyl acetate) and poly(methyl acrylate) by Fujita and Kishimoto,[59] and for nylon 6 monofilament by Dunell and Quistewater.[60] Fujita and Kishimoto measured the stress relaxation of these polymers immediately after the quick stretching, during which the water vapor was supplied from the reservoir. They obtained the master curves and shift factors for the relaxation moduli. Dunell and Quistewater measured the dynamic tensile modulus at the various relative humidity and obtained the master curve of nylon 6, similarly to our case. But, in their case the quantitative analysis of the shift factor values was not made. In the present study the dynamic Young's modulus (E' and E'') was measured for nylon 6 film under precise control of the stepwisely-scanned humidity atmosphere and the master curves could be obtained successfully as functions of systematically changed strain frequency.

The evaluated shift factor a is plotted against relative humidity as shown in Figure 18. This curve can be interpreted reasonably on the basis of the free volume change induced by the absorbed water, as discussed by Fujita and Kishimoto. According to the Doolittle viscosity equation[61] modified by Williams, Landel, and Ferry, a steady-flow viscosity η is given as[62]

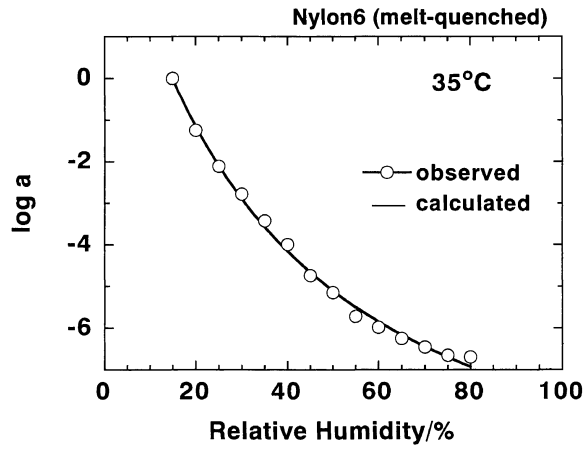

Figure 18. Relative humidity dependence of logarithmic shift factor obtained for nylon 6 film. The open circles are the observed data. The solid line is the theoretical curve calculated by eq 8 in the text.

$$\ln \eta = \ln A + B/f \tag{3}$$

where f is the fractional free volume of the system and A and B are parameters dependent on the substance. B is assumed to be equal to unity. The f is assumed to depend on the temperature and humidity, and then we have the following equations.

at the relative humidity X_{RH} and temperature T,

$$\ln \eta = \ln A + 1/f(T, X_{RH}) \quad (4)$$

at the relative humidity $X_{RH}=0$ and temperature T,

$$\ln \eta_o = \ln A + 1/f(T, 0) \quad (5)$$

For the swollen polymer system, the η is expressed as below.

$$\eta = \eta_o a [1+(\rho_p/\rho_w)C]^{-1} \approx \eta_o a \qquad (\text{for } C \ll 1) \quad (6)$$

where ρ_p and ρ_w are the densities of dried polymer and water, respectively, and C is the concentration of absorbed water which is assumed to be low. From eqs 4—6 we have

$$\ln a = 1/f(T, X_{RH}) - 1/f(T, 0) \quad (7)$$

Fujita and Kishimoto assumed that the free volume increases linearly with an increase of water content. In the case of nylon 6 film, we set the standard state to the film at 15 RH%. Therefore we have the following equation.

$$f(T, X_{RH}) = f(T, 0) + k(X_{RH} - X_{RH}^0) \quad (8)$$

where X_{RH}^0 is the relative humidity of the standard state and k is the proportional coefficient. Therefore, eq 7 is expressed as below.

$$\ln a = 1/[f(T, 0) + k(X_{RH} - X_{RH}^o)] - 1/f(T, 0) \quad (9)$$

This equation was found to reproduce the observed curve of Figure 17 quite well. The obtained parameters are as follows.

$f(T, 0)=0.036$, $k=0.078\times10^{-2}$ RH%$^{-1}$, and $X_{RH}^o=$ 15.0 RH%

According to the textbook of Ferry,[63] free volume fraction is about 0.025 at the glass transition temperatures of many amorphous polymers. The value 0.036 evaluated for nylon 6 sample is a little larger than 0.025. By absorbing water, the glass transition temperature of nylon 6 is said to decrease from *ca.* 80℃ (for dried state) to 20—30℃ (for 50% RH).[64] One of the reasons for larger value of free volume fraction may come from such a situation that the glass transition temperature is reduced by absorbing water and the measurement temperature 35℃ is above the glass transition temperature, resulting in higher mobility of the amorphous chain segment. But the value $f(T, 0)$ is for the perfectly dried state of the sample or for the sample with higher glass transition temperature of *ca.* 80℃. In this meaning, an interpretation of larger free volume fraction on the basis of the change in glass transition temperature is a little difficult to accept. Rather we may say that the sample with low degree of crystallinity contains many voids, which may contribute to increase the free volume fraction in the amorphous region. We are now investigating the humidity dependence of shift factor for many water-absorbable polymers and trying to evaluate their free volume fractions. A systematic interpretation of these data might give us any answer for the large value of free volume fraction of nylon 6 sample.

By the way, free volume fraction can be expressed as a function of temperature as follows.[59]

$$f(T, 0) = f(T_g^o, 0) + \alpha(T - T_g^o) \quad (10)$$

$$f(T, X_{RH}) = f(T_g^o, 0) + \alpha(T - T_g(X_{RH})) \quad (11)$$

where T_g^o is the glass transition temperature of the dried polymer and α is the thermal expansivity. Equation 11 was given by Fujita and Kishimoto and indicates the free volume equation at a glass transition point and at the relative humidity X_{RH}. The temperature in the dynamic modulus experiment was 35℃, which was in the region of glass transition temperature at the frequency 10 Hz of nylon 6 with low crystallinity and with small amount of absorbed water.[65,66] In this situation we may combine eqs 8, 10, and 11 together, and we have

$$f(T, X_{RH}) = f(T_g^o, 0) + \alpha(T - T_g^o) + k(X_{RH} - X_{RH}^o) \quad (12)$$

This equation is quite suggestive: the increasing temperature and the increasing humidity give the similar effect on the Young's modulus of nylon 6 film. Actually almost comparable decrement of the Young's modulus was observed in the temperature region of 30—50℃ at about 30 RH% in the "temperature dispersion" measurement, which will be reported elsewhere.

In the preceding section it was pointed out that the crystalline phase was affected more or less by absorbing water, as seen in Figure 15. If the mechanical property of the crystalline phase is changed by absorbing water, this change may influence the mechanical property of the bulk sample and therefore the frequency dispersion of the Young's modulus and the shift factor may be affected also. It must be noticed again here that the above-mentioned interpretation of the humidity-dependent shift factor on the basis of the free volume fraction in the amorphous phase was made under the assumption that the mechanical property of the crystalline region was not changed essentially even when the structure and/or the molecular motion was affected slightly by the absorbed water. A successful construction of master curves of E' and E'' may support a reasonableness of this assumption.

CONCLUSIONS

In the present paper we reported the humidity dependence of the infrared spectra and dynamic viscoelastic property of nylon 6 films with the various crystallinity by means of an organizedly combined system of FT-IR and dynamic viscoelastometer operated under the controlled humidity scanned at a constant rate. The modulus E' decreased remarkably with increasing humidity, which was interpreted successfully on the basis of the complex mechanical model with the softening of

the amorphous phase taken into consideration. The infrared spectral data gave us the information on the relative content of the absorbed water, whose change was found to have a good correlation with the change in the mechanical property. Absorbed water was considered to enter mainly into the amorphous region, the infrared bands of the crystalline region were found to change also by absorbed water: the softening of the hydrogen bonds and the conformational disordering of the chains were speculated to occur as an effect of absorbed water.

Since the present viscoelastometer can change the relative humidity in an arbitrary manner, we applied this system to measure the frequency dependence of dynamic modulus under the stepwisely-controlled humidity environment. The data could be reduced quite well to the master curves of E' and E'', indicating the possibility of time-humidity superposition principle. This principle was proposed already for several polymers, and we could confirm it by carrying out the precise measurement of frequency dispersion for the dynamic modulus (E' and E'') of the smicrystalline nylon 6 film under an exactly controlled step-scan mode of relative humidity. The evaluated shift factor could be expressed as a function of humidity, from which the humidity dependence of the free volume fraction of the amorphous region could be derived.

In this way the present system built by the combination of FT-IR and dynamic viscoelastometer under the arbitrarily controlled humidity condition is quite powerful to investigate the effect of moisture on the structure and mechanical property of polymer materials. We are now investigating this moisture effect for the various kinds of polymers in order to understand the structure-property relationship from both the microscopic and macroscopic points of view.

REFERENCES

1. H. W. Starkweather, Jr., in "Nylon Plastics", I. M. Kohan, Ed., John Wiley & Sons, Inc., New York, N.Y., 1973, chapt. 9.
2. R. Puffr and J. Sebenda, *J. Polym. Sci., C*, **16**, 79 (1967).
3. C. Vergelati, A. Imberty, and S. Perez, *Macromolecules*, **26**, 442 (1993).
4. L. E. Govaert, P. J. de Vries, P. J. Fennis, W. F. Nijenhuis, and J. P. Keustermans, *Polymer*, **41**, 1959 (2000).
5. G. T. Fieldson and T. A. Barbari, *Polymer*, **34**, 1146 (1993).
6. K. Bouma, G. de Wit, J. H. G. Lohmeijer, and R. J. Gaymans, *Polymer*, **41**, 3965 (2000).
7. H. J. Marrinan and J. Mann, *J. Appl. Chem.*, **4**, 204 (1954).
8. V. J. Frilette, J. Hanle, and H. Mark, *J. Am. Chem. Soc.*, **70**, 1107 (1948).
9. R. Ravindra, R. Kameswara, R. Krovvidi, A. A. Khan, and A. K. Rao, *Polymer*, **40**, 1159 (1999).
10. R. M. Hodge, G. H. Edward, and G. P. Simon, *Polymer*, **37**, 1371 (1996).
11. J. Pritchard, "Poly(vinyl alcohol): Basic Properties and Uses", Gordon and Breach, London, 1970.
12. N. Peppas and E. Merrill, *J. Appl. Polym. Sci.*, **20**, 1457 (1976).
13. N. Peppas, *Makromol. Chem.*, **178**, 595 (1977).
14. R. Iwamoto, M. Miyata, and S. Mima, *J. Polym. Sci., Part B: Polym. Phys.*, **17**, 1507 (1979).
15. M. Notomi, T. Miyagawa, K. Kishimoto, and T. Koizumi, *Nippon Kikai Gakkai Ronbunshu*, **59**, 422 (1993).
16. L-T. Lim, I. J. Britt, and M. A. Tung, *J. Appl. Polym. Sci.*, **71**, 197 (1999).
17. D. J. Skrovanek, S. E. Howe, P. C. Painter, and M. M. Coleman, *Macromolecules*, **18**, 1676 (1985).
18. P. E. Bretz, R. W. Hertzberg, J. A. Manson, and A. Ramirez, in "Water in Polymers", ACS Symposium Series, S. P. Rowland, Ed., American Chemical Society, Washington, D.C., 1980, pp 531—553.
19. H. W. Starkweather, in "Water in Polymers", ACS Symposium Series, S. P. Rowland, Ed., American Chemical Society, Washington, D.C., 1980, pp 433—440.
20. D. G. Hunt and M. W. Darlington, *Polymer*, **21**, 502 (1980).
21. D. G. Hunt and M. W. Darlington, *Polymer*, **19**, 1977 (1978).
22. B. Meredith and B. S. Hsu, *J. Polym. Sci.*, **61**, 253 (1962).
23. W. H. Howard and M. L. Williams, *Text. Res. J*, **36**, 691 (1966).
24. B. Bhushan and D. Connolly, *ASLE Trans.*, **29**, 489 (1986).
25. R. Bianchi, P. Chiavacci, R. Vosa, and G. Guerra, *J. Appl. Polym. Sci.*, **43**, 1087 (1991).
26. E. P. Kalutskaya and S. S. Gusev, *Vysokomol. Soedin. Ser. A.*, **22**, 497 (1980).
27. K. Nakamura, T. Hatakeyama, and H. Hatakeyama, *Text. Res. J.*, **51**, 607 (1981)
28. T. Hatakeyama, Y. Ikeda, and H. Hatakeyama, *Makromol. Chem.*, **188**, 1975 (1987).
29. T. Yorozuki and T. Ogiwara, *Kogyo Kagaku Zasshi*, **63**, 1457 (1960).
30. T. Hongo, T. Kozumi, C. Yamane, and K. Okajima, *Polym. J.*, **28**, 1077 (1996).
31. T. Ii, "Abstract of 16th Technical Committee, the Japan Adhesive Tapes Maker's Association", 1995, p 30.
32. S. Yano, M. Kodomari, and N. Okubo, "Abstract of 41st Symposium of Rheology Society of Japan", 1993, p 311.
33. H. Ichimura, T. Nakamura, R. Kinoshita, and N. Nakamura, 33rd Netsu Sokutei Symposium, 1997, p 178.
34. H. Kato, T. Nakamura, and N. Okubo, *Netsu Sokutei*, **26**, 56 (1999).
35. K. Tashiro, Y-L. Liu, and T. Ii, *Polym. Prepr., Jpn.*, **45**, 3322 (1996).
36. K. Tashiro, Y-L. Liu, H. Shirataki, T. Hongo, C. Yamane, and T. Ii, *Polym. Prepr., Jpn.*, **47**, 861 (1998).
37. K. Tashiro and S-M. Zhou, "Abstract of 19th ACS National Meeting", San Francisco, Cell, 108 (2000).
38. S. Zhou, K. Tashiro, and T. Ii, *Fiber Prepr. Jpn.*, **55**, 100 (2000).
39. S-M. Zhou, K. Tashiro, and T. Ii, *Macromolecules*, in press.
40. M. Takayanagi, H. Harima, and Y. Iwata, *Mems. Fac. Eng., Kyushu Univ.*, **23**, 1 (1963).
41. K. Tashiro, G. Wu, and M. Kobayashi, *Polymer*, **29**, 176 (1988).
42. I. Sakurada, T. Ito, and K. Nakamae, *J. Polym. Sci., C*, **15**, 75 (1966).
43. K. Miyasaka, T. Isomoto, K. Koganeya, and K. Ishikawa, *J. Polym. Sci., Polym. Phys. Ed.*, **18**, 1047 (1980).
44. K. Tashiro and H. Tadokoro, *Macromolecules*, **14**, 781 (1981).
45. K. Nakamae, T. Nishino, K. Hata, and T. Matsumoto, *Kobunshi Ronbunshu*, **44**, 421 (1987).
46. I. Sakurada and K. Kaji, *Makromol. Chem. Suppl.*, **1**, 599 (1975).
47. M. Fukuda, M. Miyagawa, H. Kawai, N. Yagi, O. Kimura, and T. Ohta, *Polym. J.*, **19**, 785 (1987).
48. G, E. Walrafen, in "Water: A Comprehensive Treatise", F. Franks, Ed., Plenum Press, New York, N.Y., 1972, vol. 1, chapt. 5.
49. J. Kim and K. S. Kim, *J. Chem. Phys.*, **109**, 5886 (1998).
50. H. Kusanagi, *Polym. Prepr., Jpn.*, **49**, 2537 (2000).
51. S. Dasgupta and W. A. Goddard, III, *J. Chem. Phys.*, **90**, 7207 (1989).
52. N. S. Murthy, M. Stamm, J. P. Sibilia, and S. Krimm, *Macromolecules*, **22**, 1261 (1989).
53. D. R. Holmes, C. W. Bunn, and D. J. Smith, *J. Polym. Sci.*, **17**, 159 (1955).
54. H. Arimoto, M. Ishibashi, M. Hirai, and Y. Chatani, *J. Polym. Sci., A*, **3**, 317 (1965).
55. H. Arimoto, *J. Polym. Sci., A*, **2**, 2283 (1964).
56. I. Sandeman and A. Keller, *J. Polym. Sci.*, **19**, 401 (1956).
57. J. Jakes and S. Krimm, *Spectrochimica. Acta*, **27A**, 19 (1971).

58. C. Ramesh and K. Tashiro, to be published.
59. H. Fujita and A. Kishimoto, *J. Polym. Sci.*, **28**, 547 (1958).
60. B. A. Dunell and J. M. R. Quiswater, *J. Chem. Phys.*, **29**, 450 (1958).
61. A. K. Doolittle and D. B. Doolittle, *J. Appl. Phys.*, **28**, 901 (1957).
62. M. L. Williams, R. F. Landel, and J. D. Ferry, *J. Am. Chem. Soc.*, **77**, 3701 (1955).
63. J. D. Ferry, "Viscoelastic Properties of Polymer", John Wiley & Sons, Inc., New York, N.Y., 1961.
64. J. Brandrup, E. H. Immergut, and E. A. Grulke, Ed., "Polymer Handbook" 4th ed, John Wiley & Sons, Inc., New York, N.Y., 1999.
65. A. E. Woodward, J. M. Crissman, and J. A. Sauer, *J. Polym. Sci.*, **44**, 23 (1960).
66. T. Kawaguchi, *J. Appl. Polym. Sci.*, **2**, 56 (1959).